

Supporting Information

Photoluminescence property of quinary Ag-(In,Ga)-(S,Se) quantum dots with a gradient alloy structure for *in vivo* bioimaging

Nurmanita Rismaningsih,^a Hiroki Yamauchi,^a Tatsuya Kameyama,^a Takahisa Yamamoto,^a Saho Morita,^a Hiroshi Yukawa,^{a,b,c} Taro Uematsu,^d Yoshinobu Baba,^{a,b,c} Susumu Kuwabata,^d and Tsukasa Torimoto^{a,b*}

^a Graduate School of Engineering, Nagoya University, Chikusa-ku, Nagoya 464-8603, Japan

^b Institute of Nano-Life-Systems, Institutes of Innovation for Future Society, Nagoya University, Chikusa-ku, Nagoya 464-8603, Japan

^c Institute for Quantum Life Science, Quantum Life and Medical Science Directorate, National Institutes for Quantum and Radiological Science and Technology, Inage-ku, Chiba 263-8555, Japan.

^d Graduate School of Engineering, Osaka University, 2-1 Yamada-oka, Suita, Osaka 565-0871, Japan

E-mail: torimoto@chembio.nagoya-u.ac.jp

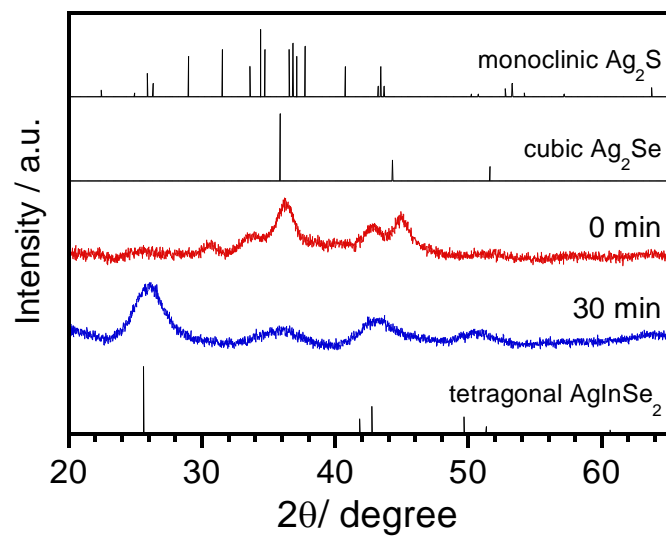


Figure S1. XRD patterns of particles shown in Fig. 1a.

Table S1. Chemical composition of AIGSSe QDs prepared with various Se/(S+Se) ratios in the precursor.

Se/(S+Se) in preparation	Composition (atom %)				
	Ag	In	Ga	S	Se
0	10.8	7.2	44.5	37.5	0.0
0.03	11.2	7.6	47.5	32.8	1.0
0.07	11.0	7.0	48.2	31.5	2.4
0.14	10.1	6.9	48.3	30.2	4.6
0.50	10.5	7.5	48.2	18.4	15.4
1.0	20.3	12.6	19.2	2.0	45.9

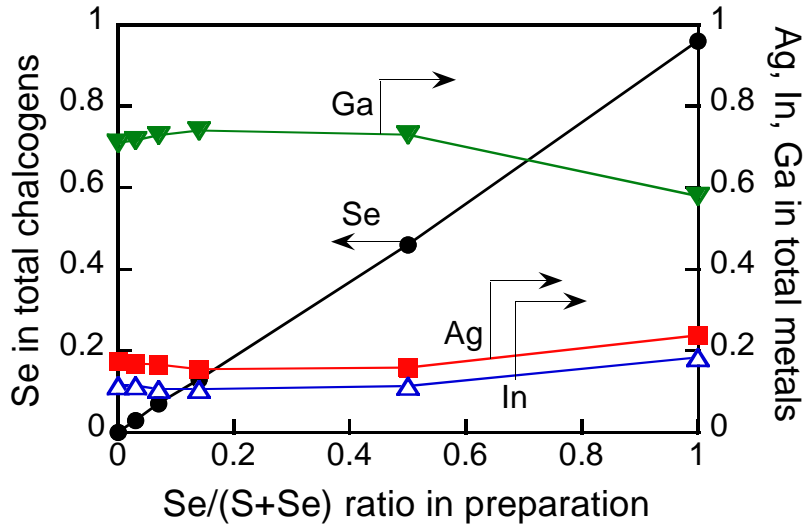


Figure S2. Changes in the Se fraction in total chalcogen atoms and the fractions of Ag, In, and Ga in total metal atoms in AIGSSe QDs prepared with different ratios of Se/(S+Se) in precursors. The data in Table S1 were used for the calculation.

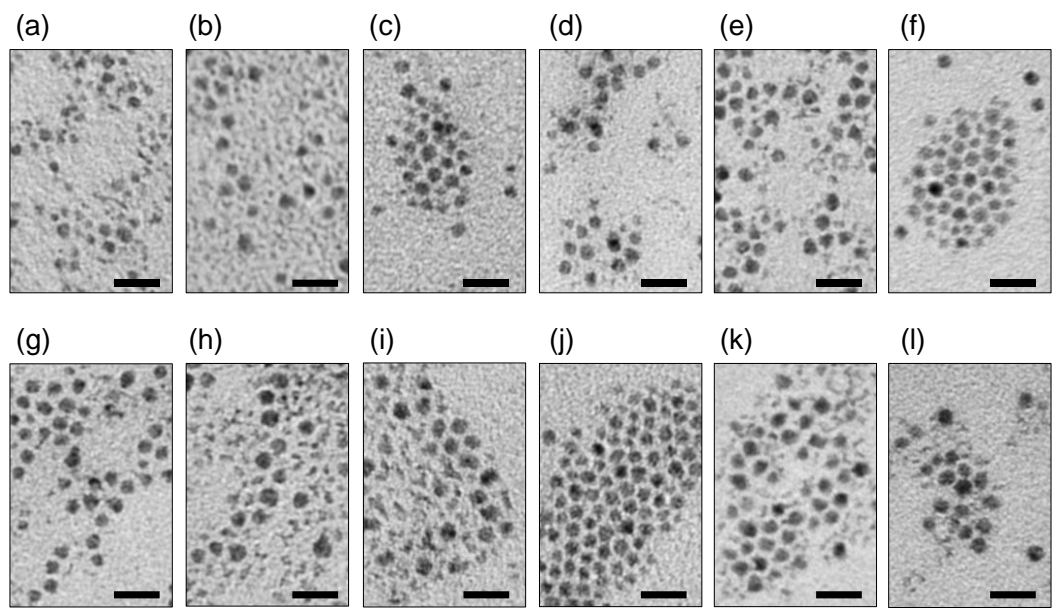


Figure S3. Wide-area TEM images of AIGSSe QDs (a-f) and AIGSSe@GaS_x QDs (g-l). Samples were prepared with Se/(S+Se) ratios of 0 (a, g), 0.03 (b, h), 0.07 (c, i), 0.14 (d, j), 0.50 (e, k), and 1.0 (f, l). Scale bars in panels represent a length of 20 nm.

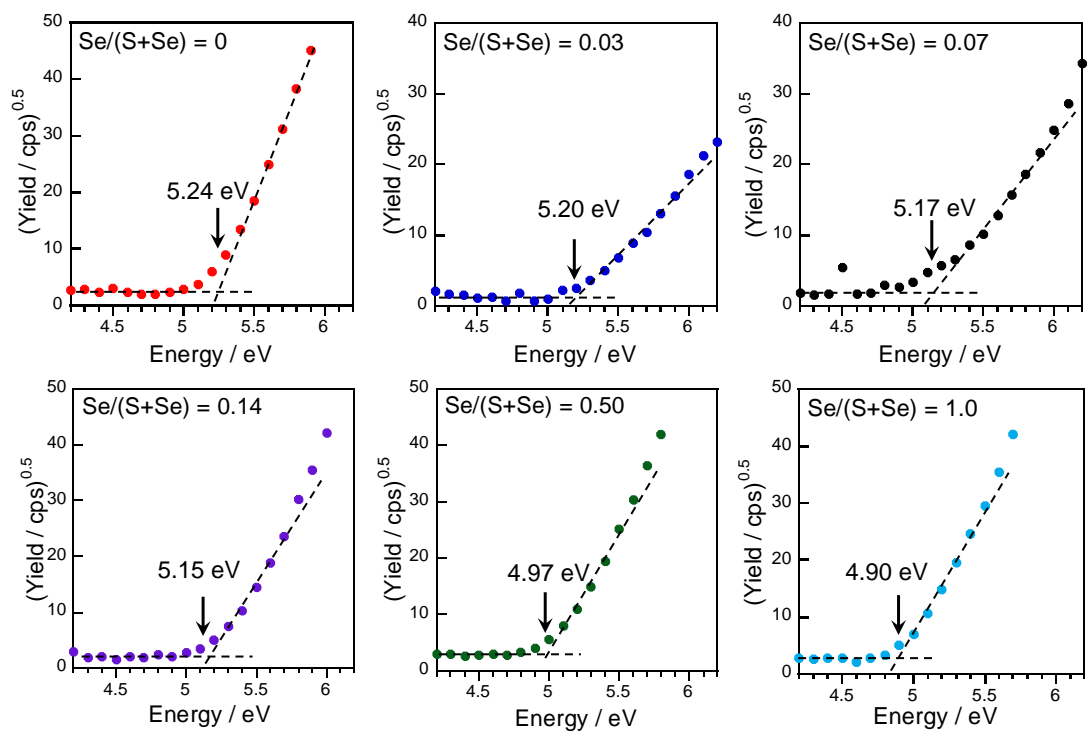


Figure S4. Representative photoelectron yield spectra of AIGSSe QDs prepared with various $\text{Se}/(\text{S}+\text{Se})$ ratios.

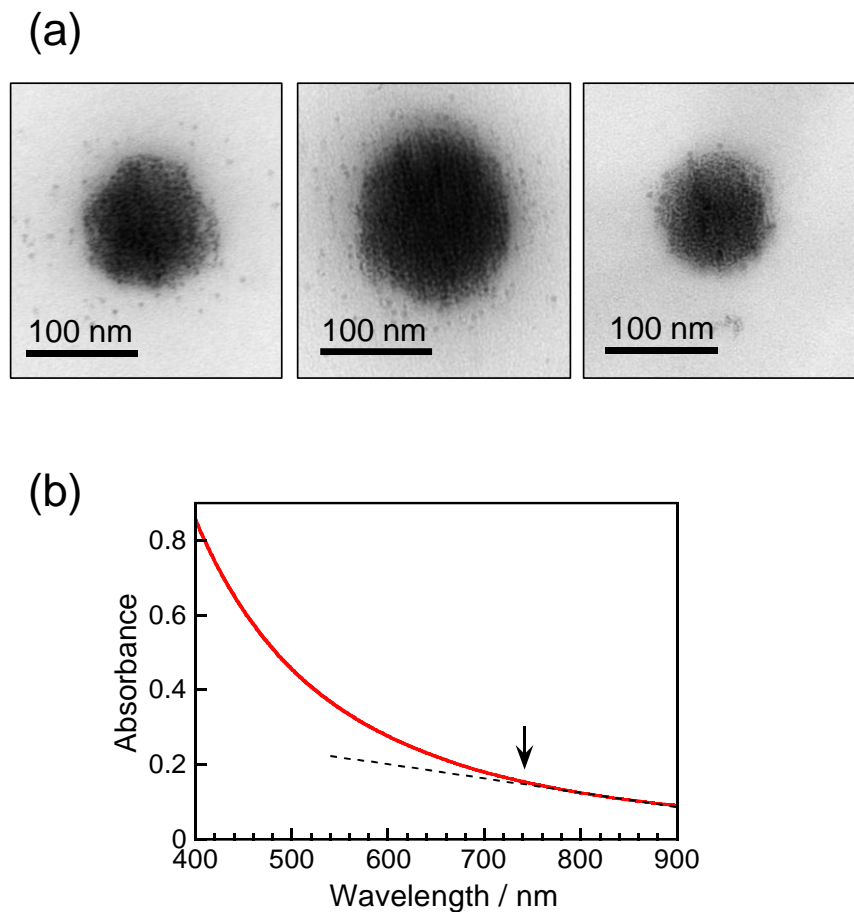


Figure S5. Typical TEM images (a) and absorption spectrum (b) of DSPC-AIGSSe@GaS_x liposomes prepared with Se/(S+Se) = 0.50. The baseline arising from the scattering of DSPC liposomes in an aqueous solution is indicated by a broken line, and the onset wavelength of the absorption by the composite is indicated by an arrow in the panel b.

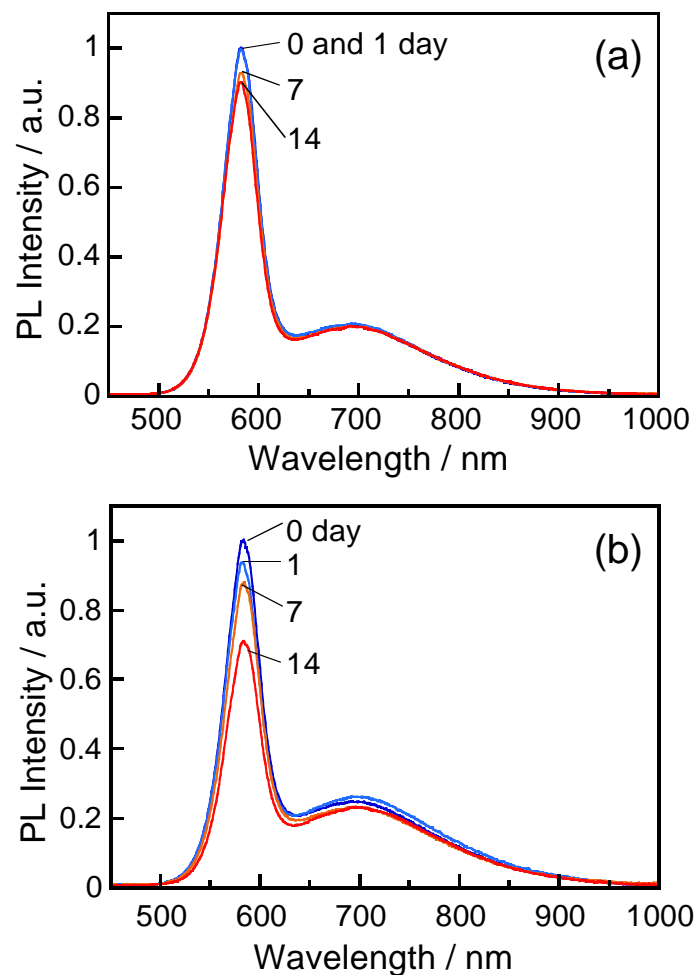


Figure S6. Changes in PL spectra of DSPC-AIGSSe@GaS_x ($\text{Se}/(\text{S}+\text{Se}) = 0$) aqueous dispersions stored in the dark under an N₂ atmosphere (a) and in air (b).

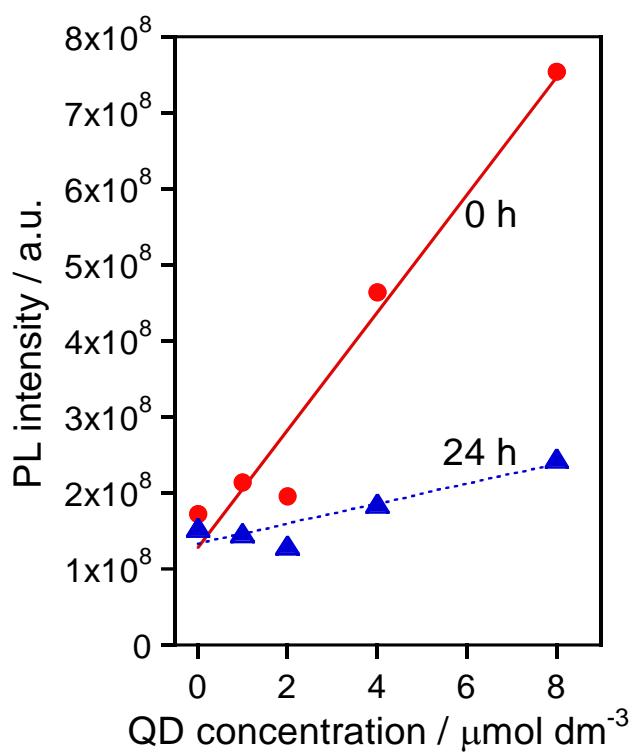


Figure S7. Relationships between the PL intensities detected at 0 and 24 h through the skin of the mouse and the QD concentration in DSPC-AIGSSe@GaS_x (Se/(S+Se)= 0.50) liposome dispersions injected.

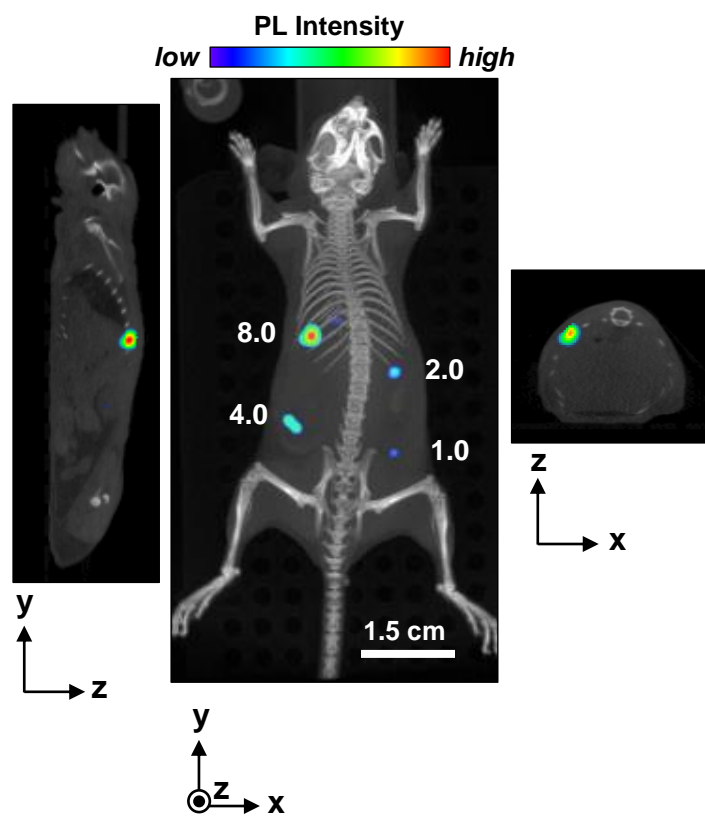


Figure S8. A three-dimensional PL image superimposed on an X-ray CT image of the mouse subcutaneously injected with DSPC-AIGSSe@GaS_x liposome dispersions in the back. A top view (center) and cross-sectional views of y-z (left) and x-z planes (right). The numbers in the center panel represent the concentrations of QDs in the dispersions in the unit of $\mu\text{mol}(\text{QDs}) \text{dm}^{-3}$.

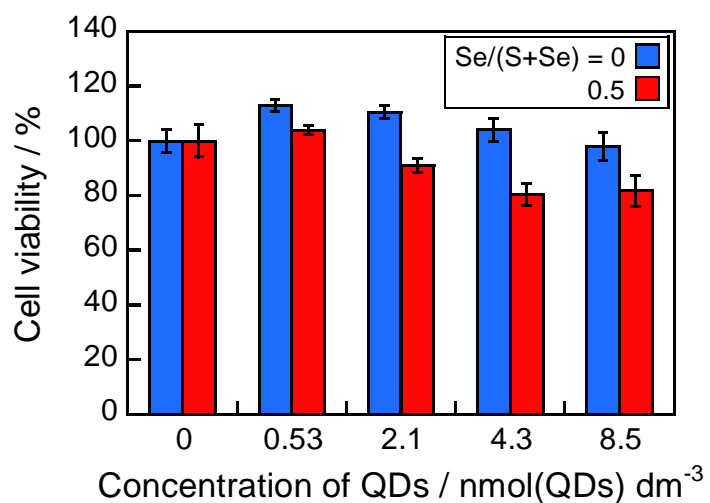


Figure S9. Concentration dependence of the viability of A431 cells exposed for 24 h to DSPC-AIGSSe@GaS_x liposomes. The QDs used are those prepared with Se/(S+Se) = 0 (blue bars) and 0.50 (red bars).